MOLECULAR IMAGING AND BIOLOGY

Published Online: 8 April 2010

Mol Imaging Biol (2010) 12:595–607
DOI: 10.1007/s11307-010-0305-1

RESEARCH ARTICLE

Folate-Polyethylene Glycol Conjugated Near-Infrared Fluorescence Probe with High Targeting Affinity and Sensitivity for *In Vivo* Early Tumor Diagnosis

Fei Liu,[1] Dawei Deng,[1] Xinyang Chen,[1] Zhiyu Qian,[2] Samuel Achilefu,[3] Yueqing Gu[1]

[1]*Department of Biomedical Engineering, School of Life Science and Technology, China Pharmaceutical University, Nanjing 210009, People's Republic of China*

[2]*Department of Biomedical Engineering, School of Automation, Nanjing University of Aeronautics and Astronautics, Nanjing 210016, People's Republic of China*

[3]*Department of Radiology, School of Medicine, Washington University, St. Louis MO, USA*

Abstract

Purpose: The purpose of this study is to synthesize a folate-polyethylene glycol (PEG) conjugated near-infrared fluorescence probe (fPI-01) for diagnosis of folate receptor (FR)-overexpressed tumors with high sensitivity and specificity.

Procedures: fPI-01 was synthesized, purified, and characterized. Its cytotoxicity and affinity to tumor cells were determined *in vitro*. The dynamics and biodistribution of the probe was monitored in normal nude mice. And the tumor-targeting capability was investigated in nude mice bearing different tumor xenograft.

Results: fPI-01 was successfully synthesized with strengthened optical properties. Cells experiments showed the probe had high FR affinity and without apparent cytotoxicity. Animal experiments indicated the probe excreted through urine by kidney. And its tumor-targeting ability was demonstrated on different tumor-bearing mice, with high sensitivity and tumor-to-normal tissue contrast ratio (10:1).

Conclusions: fPI-01 is a promising optical agent for diagnosis of FR-positive tumors, especially in their early stage.

Key words: Folate, Near-infrared fluorescence imaging, Tumor, Diagnosis

Abbreviations FR folate receptor; PEG polyethylene glycol; DCC 1-(3-dimethylaminopropyl)-3-ethylcarboiimide; NHS N-hydroxysuccinimide; TLC thin layer chromatography; MTT 3-(4,5-dimethylthialzol-2-yl)-2,5-diphenyl tetrazolium bromide; CCD charge-coupled device; NIR near infrared

Its significance: A folate receptor-targeted near-infrared fluorescence probe (folate-PEG-ICG-Der-01 probe, fPI-01) was synthesized with strengthened fluorescence intensity and photostability. The satisfactory targeting capability for folate receptor-overexpressed tumors was demonstrated in different tumor-bearing mice. The PEG_{4000} conjugation did improve the dynamics of the probe in mice subjects and enhance the targeting capability and sensitivity to FR-overexpressed tumors. Results in our study indicated the probe possesses great potential in the diagnosis of early stage tumors.

Correspondence to: Yueqing Gu; *e-mail:* guyueqing@hotmail.com

Introduction

The folate receptor (FR), known as the folate-binding protein with a naturally 38-kDa glycopolypetide, is overexpressed in many cancer cells, including cancers of the ovary, kidney, uterus, testis, brain, colon, lung, and hematopoietic cells of myelogenous origin [1]. Since the folate receptor-mediated endocytosis was firstly discovered

by Leamon and Low in Purdue University in 1991, folic acid, a high affinity ligand to the folate receptor, has emerged as an optimal targeting warhead for selective delivery of attached imaging and therapeutic agents to carcinomas and inflammation [2]. Folic acid has been approved to retain its receptor-binding properties when being derivatized via its γ-carboxyl [3, 4]. Recently, the high affinity ($K_D \sim 10^{-10}$M) of folic acid binding with folate receptor and the endocytic mechanism of shuttling these bound molecules inside cells were completely confirmed [5]. More and more folate conjugations have been developed and used in tumor treatment and imaging, such as biodegradable polymers drug carrier [6], small radioactive imaging agents [7, 8], MRI imaging agents [9], near-infrared fluorescence imaging agents [10, 11], antineoplastic drugs [12], liposomal drug carriers [13], nanodrugs [14], gene vectors [15], and large DNA-containing formulations [16]. Most of the folate conjugations displayed better efficacy for folate-positive tumor treatment *in vitro* and diagnosis *in vivo* than that of the non-specific drugs did.

Optical imaging represents a rapidly expanding field, with direct applications in cellular biology, pharmacology, and diagnosis [17, 18]. In particular, near-infrared (NIR) fluorescence imaging possesses many advantages as a non-invasive technique for *in vivo* real-time monitoring or tracing of biological information and signals in living subjects [19, 20]. The wavelength range of NIR light is from 700 to 900 nm, avoiding the high absorption of intrinsic chromospheres such as hemoglobin, water. And thus, it can penetrate the deeper tissue of the living body without any ionizing and radioactive. Up to now, many near-infrared fluorescence dyes have been developed and used for tumor detection *in vitro* and *in vivo* [21]. Among them, ICG is the typical organic dye firstly approved by FDA to be applied into human being. Many research groups were focused on the synthesis of ICG derivatives for potential application in tumor diagnosis [22]. However, most of dyes lack the specificity for tumor tissues. Therefore, it is necessary to label them to some targeted molecules, such as antibodies [23], antibody fragments, proteins, and peptides [24, 25].

To obtain a targeting compound, more and more strategies have been aimed to label organic dyes to some ligands as optical probe to expand their application *in vivo*. However, the properties of optical imaging probes greatly depend on its components of the conjugation. Different linkers make the probes to display different dynamic properties and targeting abilities in living subjects. PEG is the additional polymers of ethylene oxide and water and their ethers. The states vary from liquid to solid with the variation of molecular weight. PEGs with different molecular weight have been widely used as surfactants in the products of foods, cosmetics, and pharmaceutics. It is also commonly applied in biomedicine served as dispersing agents, solvents, ointment and suppository bases, vehicles, and tablet excipients. PEG modification (PEGylation) in drug development is a well-established technique for therapeutic peptides and proteins to obtain high solubility, prolonged circulation, and superior biocompatibility [26, 27]. In particular, the conjugation with PEG (MW 4,000) not only reduces the endocytosis by reticuloendothelial system, but also lowers the quick filtration by renal glomerulus. PEG conjugated folate-mediated optical probe would posses higher targeting capability, and thus more potential for *in vivo* diagnosis. Though folate-conjugated near-infrared fluorescence dyes synthesized via a short PEG (EDBEA) or a hydrophilic peptide as the linkers were respectively reported by Tung and Zheng' group, PEG with molecular weight of 4,000, which is popularly used in drug development, has never been reported to link folate and the near-infrared fluorescence dyes [28, 29].

In this study, ICG-Der-01, a hydrophobic derivative of ICG synthesized in our lab by modifying Achilefu's reported method [30], was used in our probe conjugation. The maximum absorption and emission peaks of ICG-Der-01 are respectively at 783 and 808 nm in whole blood, which is within the tissue transparent window. Thus, it possesses significant potential for *in vivo* monitoring/imaging/tracing information in living body [31]. Then, PEG-bis-amine (MW 4,000), synthesized in our lab by conforming to the reported method [32], was chosen as the linker between folic acid and organic dye in the conjugation. The optical properties and photostability of the synthesized compound (folate-PEG-ICG-Der-01 probe, fPI-01) were characterized. The cytotoxicity and folate receptor affinity of the probe were investigated by *in vitro* cell experiments. The dynamics and biodistribution were examined in normal male nude mice (n=4). And the tumor-targeting capability was *in vivo* investigated in five groups of nude mice bearing different tumor xenograft by using the near-infrared fluorescence imaging system.

Materials and Methods

Materials

Folic acid (MW 441.4), N,N′-dicyclohexylcarbodiimide (DCC), N-hydroxysuccinimide (NHS), and 3-(4,5-dimethylthialzol-2-yl)-2,5-diphenyltetrazolium bromide (MTT) were purchased from Sigma-Aldrich (Shanghai, People's Republic of China). ICG-Der-01(MW 689) and PEG-bis-amine (MW 4,000) were prepared in our laboratory. RPMI 1640, folate-free RPMI 1640, fetal bovine serum, penicillin, streptomycin, and trypsin-EDTA were purchased from Gibco (Life Technologies, Shanghai, People's Republic of China). Other chemical reagents used in the study were certified analytical reagent grade (Shanghai Chemical Reagent Company, Shanghai, People's Republic of China).

Apparatus

A UV-Vis Spectrophotometer (JH 754PC, Shanghai, People's Republic of China) was used to perform the absorbance measurements. PHS-25 pH meter (Shanghai, People's Republic of China) was used to measure the pH values. Sephadex G-25 columns were used to purify the product.

A NIR spectral system was used to *in vitro* acquire the optical signals from sample. It is mainly composed of an

excitation laser (λ=765.9 nm, NL-FC-2.0-763 laser light, Enai, Shanghai) and S2000 eight-channel optical spectrographotometer (Ocean Optics), as shown in Fig. 1a.

A NIR imaging system was applied to *in vivo* real-time image the fluorescence signal from the animal subjects. This self-built imaging system was reported in our previous work, as shown in Fig. 1b [33]. In brief, the NIR imaging system is composed of an excitation laser (λ=765.9 nm, NL-FC-2.0-763 laser light), a high sensitivity NIR CCD camera (PIXIS 512B, Princeton Instrument) and an 800-nm-long pass filter for capturing the emitting fluorescence from the tissue. Besides, another HLU32F400 808 nm laser (LIMO, Dortmund, Germany) is supplied as background light to obtain the profile of the subjected animal. Otherwise, the imaging was completely dark except for the fluorescence spot.

Cell Culture

Folate receptor-positive cell lines including human cervical cancer cell line (HeLa cells), human hepatoma cell line (Bel-7402 cells, $HepG_2$ cells), rat glioma cell line (C6 cells), and folate receptor-negative cell line, human lung carcinoma cell line (A549 cells) were all purchased from ATCC (Manassas, VA, USA). These cell lines have been widely used for identification of folate-targeted complex *in vitro* [28, 34–36]. All the cell lines were cultured continuously at 37°C in a humidified atmosphere containing 5% CO_2 in folate-free RPMI 1640 medium supplemented with 10% fetal bovine serum, 100 U/ml penicillin, and 100 μg/ml streptomycin. The final folate concentration (with the fetal bovine serum as the only source of folate) falls in the range of the physiological concentration in human serum.

Animal Experiments

All animal experiments were carried out in compliance with the Animal Management Rules of the Ministry of Health of the People's Republic of China (document no. 55, 2001) and the guidelines for the Care and Use of Laboratory Animals of China Pharmaceutical University.

Athymic nude mice (nu/nu CD-1 male and female) were purchased from Charles River Laboratories (Shanghai, People's Republic of China). Four male nude mice were used to investigate the dynamic and biodistribution of fPI-01 after tail vein administration of the probe.

Tumor Models

Five kinds of tumor models were established in these female athymic nude mice according the reported methods [37] (n=4 for each group).

In detail, ~2×10^6 Bel-7402 cells were subcutaneously injected into the right axillary fossa of each mouse (n=4). After the diameter of the tumor in the group reached about 0.4 ~ 0.6 cm, they were used for fluorescence imaging to compare the targeting ability of fPI-01 with that of ICG-Der-01 dye itself.

A549 cells were subcutaneously injected into the left lower abdomen of each subject mouse. After the diameter of the tumor in the group reached about 0.4 cm, they were used for fluorescence imaging as the folate receptor-negative control *in vivo*.

HeLa cells were subcutaneously injected into the right lower abdomen of each subject mouse. After 4 days post-injection when the tumor did not form, the mice were imaged for investigation of early stage tumor detection.

Both HeLa and $HepG_2$ cells were injected into the same subject mouse (n=4), with $HepG_2$ in the right axillary fossa and HeLa at the lower abdomen of each mouse. After the diameters of the tumors grew up to ~0.6 cm ($HepG_2$) and ~0.4 cm (HeLa), respectively, they were imaged for further study of tumor-targeting capability.

C6 cells were subcutaneously injected into the left lower abdomen of each subject mouse. After the diameter of the tumors reached about 0.5 cm, they were used for fluorescence imaging.

Synthesis of Folate-PEG-ICG-Der-01 Probe

fPI-01 was synthesized in two steps. Firstly, folate-PEG-amine was synthesized by following the way as reported in the paper of Destito [38]. In brief, 22 mg of folic acid was reacted with DCC/NHS (with different feed ratio of folate:DCC:NHS) in anhydrous dimethyl sulfoxide (DMSO, 2.5 ml). After stirred in dark for 6 h at 50°C, the solution was mixed with PEG-bis-amine (MW 4,000, 1.2 equiv) dissolved in a mixture of DMSO (2.5 ml) and triethylamine (0.1 ml). The mixture was stirred at room temperature overnight in dark. The solution was first placed into MW 3,400 cutoff dialysis bags and dialyzed against deionized water to remove little side product. And the thin layer ninhydrin assay was performed to confirm the existence of $-NH_2$ group. Then folate-PEG was purified by filtration over a Sephadex G-25 column equilibrated with 0.1 M pH 7.4 PBS to

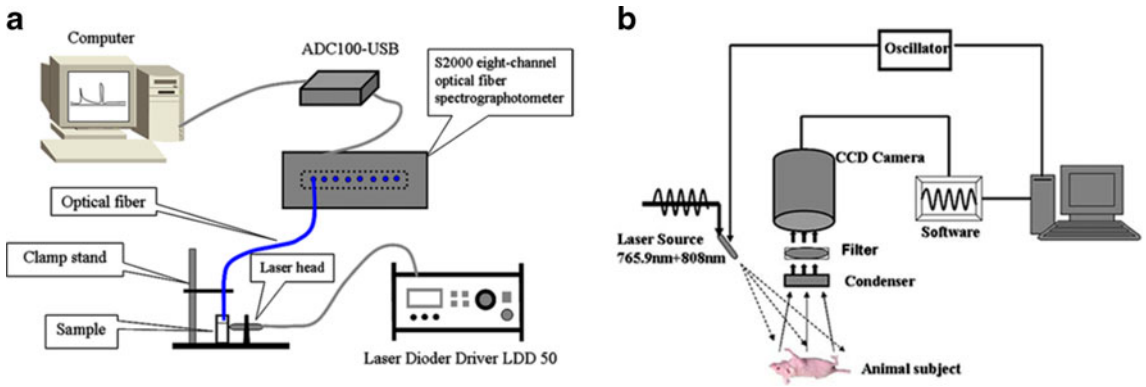

Fig. 1. Schematic diagram of NIR spectral system (**a**) and NIR imaging system (**b**).

remove unconjugated folic acid and unreacted PEG-bis-amine fragments. Fractions containing folate-PEG-NH_2 were pooled, dried under reduced pressure, and stored at −20°C. The product was determined by ultraviolet absorbance at 365 nm for folate recognition.

Near-infrared fluorescence dye, ICG-Der-01 was then conjugated with folate-PEG. In detail, ICG-Der-01 in 2 ml DMSO was added with DCC and NHS (molar ratio of ICG-Der-01:DCC: NHS=1:1.2:2), and the reaction was conducted at room temperature in dark for 2 h. And then folate-PEG-amine in 8 ml pH 9.0 carbonate buffer solution was mixed with the activated ICG-Der-01 in DMSO (molar ratio of ICG-Der-01:folate-PEG-amine=2:1). The mixture was stirred in dark for 8 h. After the mixture was dialyzed against deionized water for 2 days and lyophilized, fPI-01 was purified by filtration over a Sephadex G-25 column equilibrated with 0.1 M pH 7.4 PBS to remove unconjugated ICG-Der-01 and unreacted folate-PEG-NH_2. The synthetic diagram was shown in Fig. 2. The successful conjugate was determined by a UV-Vis Spectrophotometer. The fluorescence intensity and photo-stability were characterized, respectively.

Cytotoxicity of fPI-01

To evaluate the cytotoxicity of fPI-01, MTT assay was conducted following the standard protocol reported previously [39]. HeLa cells (180 µl) in RPMI 1640 (2×10^4 cells/ml) was added into each well in a 96-well plate and incubated for 12 h. The culture medium was replaced by 200 µl of RPMI 1640 containing fPI-01 with particular concentrations (0, 0.0625, 0.125, 0.25, 0.5, 1, and 2 µM). After 44 h, the medium with fPI-01 in each well was replaced and the cells were washed three times with PBS before addition of 180 µl fresh RPMI 1640 and 20 µl of MTT solution (5 mg/ml). After incubation for another 4 h, the medium containing MTT was slightly removed from each well and 150 µl of DMSO was added to dissolve the formed crystals. The optical density (OD) was measured at 570 and 630 nm with a multi-well plate reader (Bio-Rad, model 580). The viable rate could be calculated by the following equation: viable ration=$(OD_{treat}/OD_{control}) \times 100\%$, where OD_{treat} was obtained in the presence of fPI-01, $OD_{control}$ was obtained in the absence of fPI-01.

Determination of Folate receptor Expression on Four Kinds of Tumor Cells

Reverse-transcriptase PCR was applied to evaluate the folate receptor expression in the four tumor lines used in this study. Total RNA was extracted from freshly isolated Bel-7402, HeLa, $HepG_2$, and A549 cells using RNeasy Kit (Qiagen Inc, Valencia, CA, USA). RNA (4 µg) from each cells was converted into cDNA with Superscript™ II reverse transcriptase (Invitrogen Corp., Carlsbad, CA, USA). Then 200 ng cDNA was used for PCR amplification using folate receptor specific primers: sense, 5′-ACACCAGCCAGGAAGCCCATA-3′; antisense, 5′-GAGCAGC-CACAGCAGCATTAG-3′. The product length was 563 bp. To quantitative determination of expression, GADHP was also used in the RT-PCR. The product (10 µl) was used for 2% agarose gel electrophoresis.

Folate-Targeted Capability of fPI-01 for Tumor Cells

Folate-positive human cervical cancer cells (HeLa cells) in folate-free RPMI 1640 media and folate-negative human lung carcinoma cells (A549 cells) in normal RPMI 1640 media were cultivated for investigating the targeting function of the probe. The cells were plated in a 96-well cell culture plate at a density of 2.5×10^5 cells/well and allowed to grow for 12 h before the treatment. Then, the medium was replaced with 200 µl of fresh medium without folic acid and serum, but with various concentrations of fPI-01. The fPI-01 treated cells were then incubated again at 37°C for 1.5 h. The cells were washed three times with 0.05% Tween-20 of cold PBS solution to remove the free fPI-01 in the medium. At last, 100 µl of a cell lytic buffer solution was added to each well, the plate was laid under the NIR imaging system for fluorescence imaging.

Dynamics and Biodistribution of fPI-01 in Normal Male Nude Mice

Normal male nude mice were used for obtaining the dynamics of fPI-01 (n=4). The monitoring procedure followed our previous report [40]. In brief, 2 nmol of fPI-01 in 0.1 ml saline was tail vein injected into each mouse. Then, these mice were laid under the NIR imaging system for fluorescence imaging for 8 h in a dark room. A series of images were collected from the subject mice and the background images were taken for each mouse prior to injection.

To confirm the displayed biodistribution of fPI-01 in different organs, the subject mice were performed the imaging and sacrificed at 8 h post-injection. Different organs were separated and washed by saline and put together for fluorescence imaging.

Targeting Capability of fPI-01 Compared with ICG-Der-01 in Nude Mice Bearing Bel-7402 tumor Xenograft

Two groups of mice bearing Bel-7402 tumor xenografts were used to evaluate the tumor-targeting capability of the probe (n=4). After 2 nmol of ICG-Der-01 and fPI-01 in 0.1 ml saline was injected into each mouse of each group, these mice were laid under the NIR imaging system in a dark room for tracing the fluorescence signal. Then a series of images were collected at assigned time intervals during 48 h post-injection. Background images were taken for each mouse prior to probe injection.

Determination of fPI-01 in Nude Mice Bearing Folate Receptor-Negative A549 Tumor Xenograft

To further determine the folate receptor-targeting ability of fPI, the folate receptor-negative A549 cells were also implanted in nude mice (n=4). After fPI-01 in 0.1 ml saline was injected into each mouse, these mice were monitored under the NIR imaging system for 24 h.

Targeting Sensitivity of fPI-01 in Little Unformed HeLa Tumor Models In Vivo

To investigate high targeting sensitivity of fPI-01 *in vivo*, nude mice bearing little unformed HeLa tumor was studied by NIR imaging (n=4). Four days after HeLa cells implantation when the tumor did not form, the mice were used to determine whether the

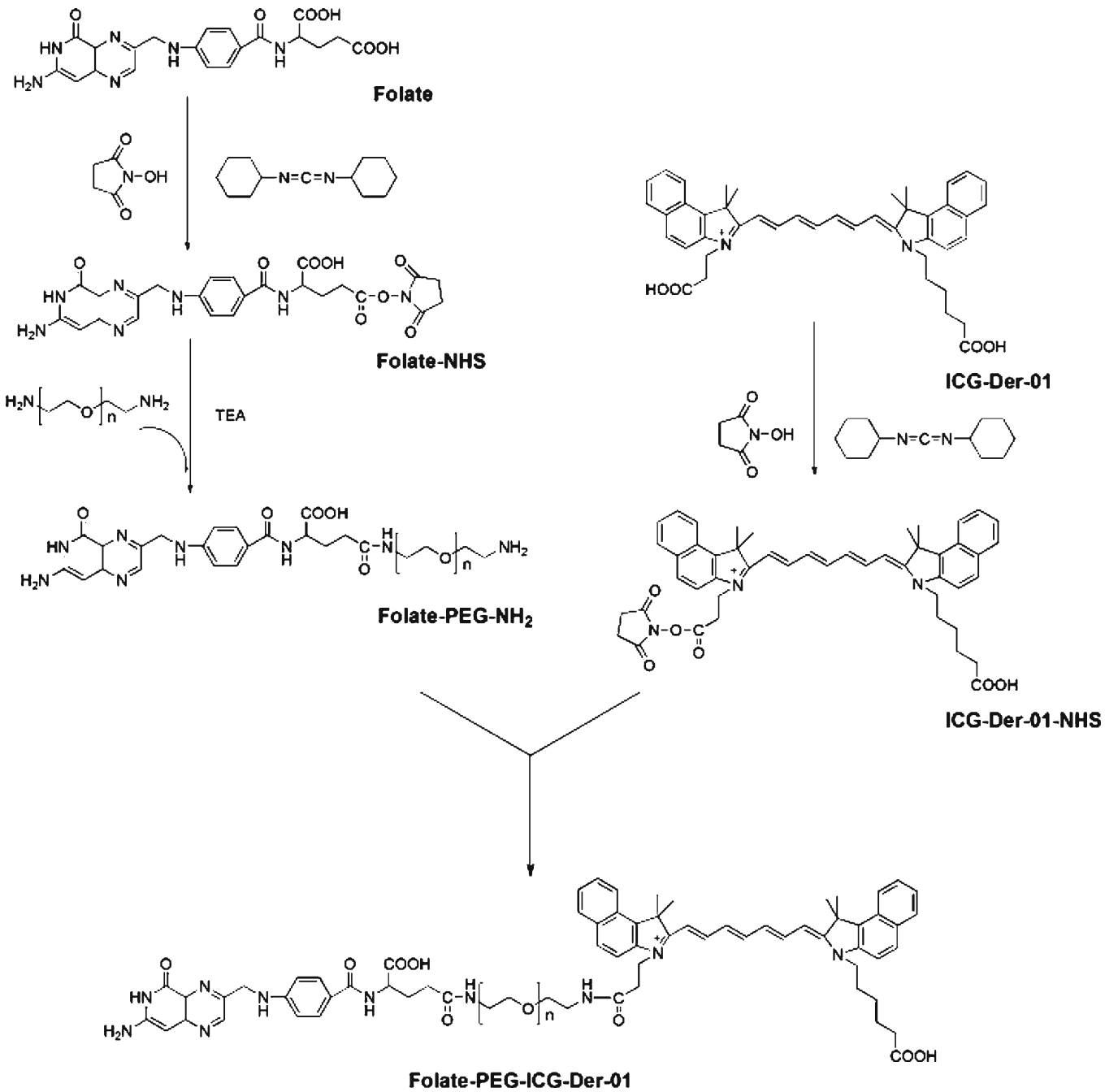

Fig. 2. Synthesis of Folate-PEG-ICG-Der-01 Probe (fPI-01).

probe could recognize the little unformed tumor. After 2 nmol of fPI-01 in 0.1 ml saline was injected into each mouse, they were imaged by NIR imaging system at different time intervals.

Targeting Diagnosis of fPI-01 in Nude Mice Bearing C6, Both $HepG_2$ and HeLa Tumor Xenografts

Two groups of nude mice respectively bearing C6, both $HepG_2$ and HeLa tumor xenograft were used for tumor diagnosis *in vivo* (n=4 for each group). After 2 nmol of fPI-01 in 0.1 ml saline was injected into each mouse, these mice were laid under the NIR imaging system in a dark room. Then a series of images were collected at assigned time intervals from 0 to 24 h post-injection.

Results

Synthesis of fPI-01

In our study, the unprotected folic acid was used to conjugate with PEG-bis-amine in our synthesis to precede the γ-carboxyl be activated. The different molar ratio of DCC and NHS was used to prohibit the activation of α-carboxyl group. And the product was compared and

characterized by TLC. Fig. 3 depicted that the scheme (a) of folate:DCC:NHS=1:1.2:2 for carboxyl activation only produce one bright spot except the folic acid itself, while the scheme (b) of folate:DCC:NHS=1:2:2 yielded two obvious bright spots, with both γ- and α-carboxyl activated. The scheme (a) (1:1.2:2) was considered as the optimal condition of DCC and NHS. PEG_{4000}-bis-amine was chosen as the linker between folic acid and the near infrared dye for its pharmacokinetic and immunological advantages *in vivo* [41]. As described in "Materials and Methods" section, folate was conjugated to PEG_{4000}-bis-amine and the product was subsequently characterized by thin layer ninhydrin assay. It was shown that the existence of $-NH_2$ of folate-PEG (data not shown here). The purified folate-PEG was also characterized by absorption spectrum analysis, as shown in Fig. 4a. The absorption spectrum of folic acid and folate-PEG was almost the same in pH 7.2 PBS (absorption peaks at 280 and 365 nm). The spectrum of folate was not affected when it was conjugated with PEG_{4000}-bis-amine.

Then, near infrared dye ICG-Der-01 was conjugated with folate-PEG-NH_2 in the same way as folate was conjugated with PEG_{4000}-bis-amine. The absorption spectra of the purified product, fPI-01 was plotted along with the ICG-Der-01 dye, as shown in Fig. 4b. The absorption peaks showed the coexistence of both folic acid (absorption peaks at 280 and 365 nm) and ICG-Der-01 (absorption peak at 783 nm). It was inferred that the synthesized probe concurrently composed of folate and ICG-Der-01.

The fluorescence intensity of fPI-01 and ICG-Der-01 dye was compared, as shown in Fig. 4c. fPI-01 and ICG-Der-01 with same molar concentration of dye were dissolved in pH 7.2 PBS. The fluorescence was acquired by the NIR spectral system with the excitation at 765.9 nm. Results in Fig. 4c indicated that fPI-01 showed much higher fluorescence intensity than that of ICG-Der-01.

The photostability of the probe was also characterized by NIR spectral system. The fluorescence intensity was collected at different time internals during the continuous exposure of probe to the exaction light at 765.9 nm. Fig. 4d displayed the normalized fluorescence intensity of fPI-01 and ICG-Der-01. The normalized fluorescence intensity of fPI-01 decreased from 1 to 0.718, reduced by 28.2%, while that of ICG-Der-01 decreased from 1 to 0.459, reduced by 54.1%. It was inferred that the photostability was strengthened when ICG-Der-01 was conjugated to folate-PEG.

Cytotoxicity

MTT assay was carried out to evaluate the cytotoxicity of fPI-01 on HeLa cells. Results exhibited at least 88.2% of cell viability under all the concentrations, indicating a non-apparent cytotoxicity of fPI-01 (Fig. 5, $n=5$). More importantly, the probe concentration with good cell viability was later used for *in vivo* imaging (2 μM). The long life time of the subject mice demonstrated once again the non-toxicity of the probe to animal subject during the imaging process.

Quantitative Determination of Folate Receptor Expression on Tumor Cells

To better understand the folate-targeting mechanism of the synthesized probe, the expression levels of folate receptor on Bel-7402, A549, HeLa, and $HepG_2$ cells were investigated. Fig. 6a and b depicted the mRNA levels of folate receptor in the four kinds of tumor cells. Results showed that Bel-7402 had the highest expression level among the four tumor lines. And HeLa and $HeopG_2$ also expressed abundant folate receptor. As expected, A549 cells showed no observable expression. Thus, it can be selected as folate-negative

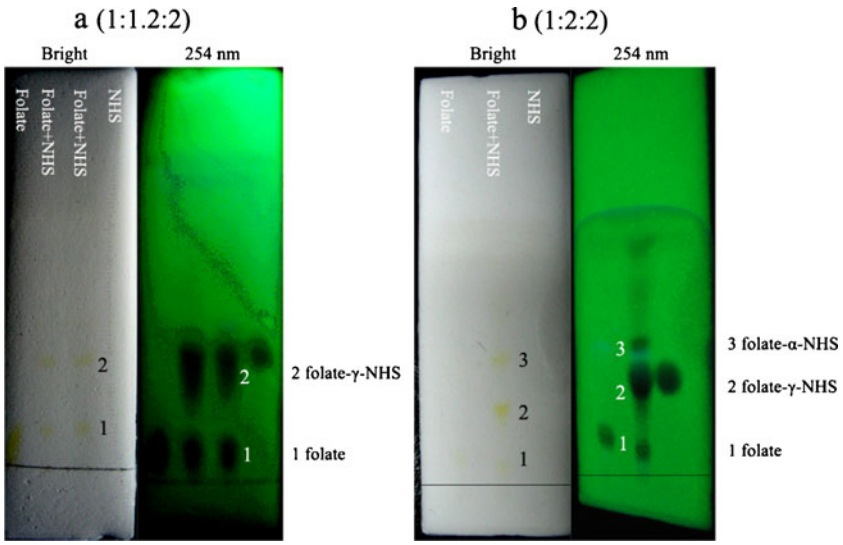

Fig. 3. Characterization of folate-NHS by TLC (chloroform:methanol:amine=6:4:1). **a** Scheme *(1:1.2:2)* displayed a main new point of folate-NHS. **b** Scheme *(1:2:2)* displayed two new points of activated folate.

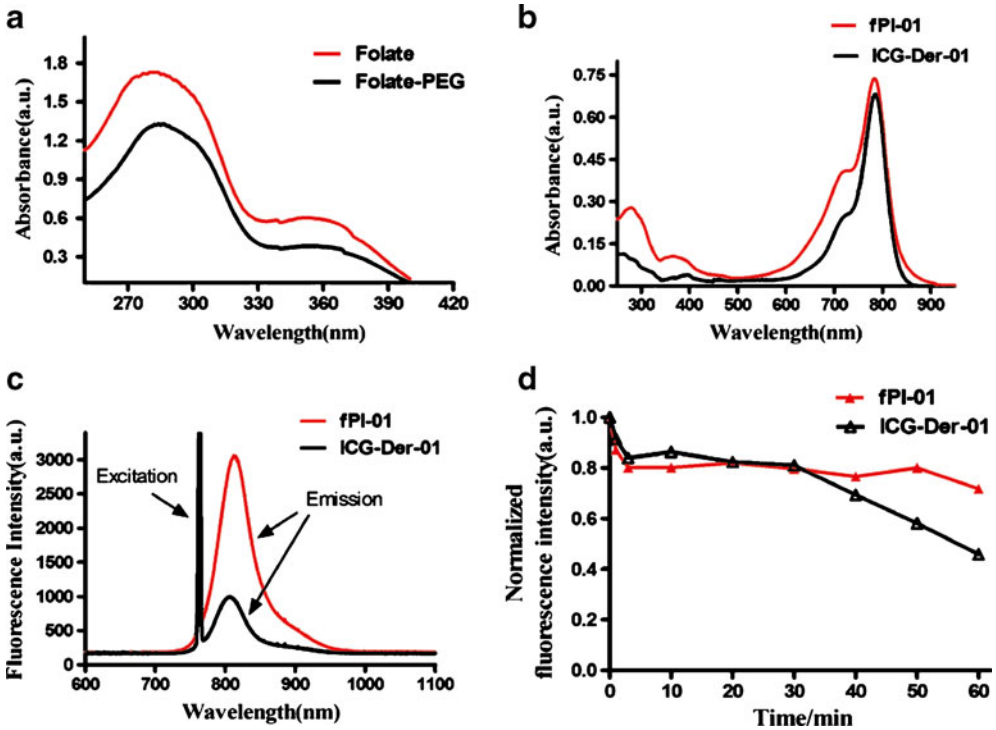

Fig. 4. **a** Relative absorption spectrum of folate and folate-PEG. The absorption peaks were at 280 and 365 nm. **b** Absorption spectrum of fPI-01 and ICG-Der-01. The absorption peaks at 280, 365, and 783 nm represent absorption by folic acid and ICG-Der-01, respectively. **c** Fluorescence spectrum of fPI-01 and ICG-Der-01, with same molar concentration of dye. The excitation peak at 765.9 nm and the emission peak of fPI-01 at 819 nm in pH 7.2 PBS. **d** Photostability of fPI-01 and ICG-Der-01.

control. The obtained results were in accord with the reference.

In Vitro Cell Targeting

HeLa and A549 cells were incubated with fPI-01 at different concentrations for 1.5 h, the fluorescence intensity was determined under NIR imaging system. As shown in Fig. 7a, the fluorescence signals from HeLa cells were higher than that from A549 cells at the same concentration. Then, the average fluorescence intensity was acquired by selecting the special region of interests in each well from the obtained image [40]. Fig. 7b presented the analyzed data of the fluorescence intensity in each well. It could be concluded that both kinds of the cells took the probe, but HeLa cells took more fPI-01 than A549 cells did.

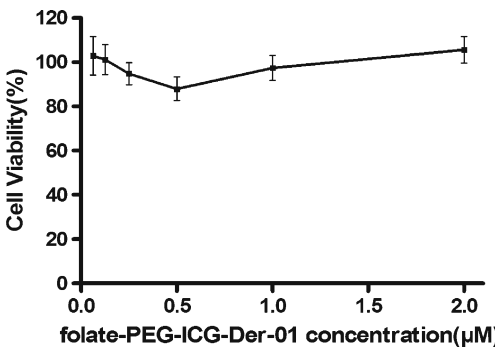

Fig. 5. Cytotoxicity study of fPI-01. Cell viability was above 88.2%.

The Dynamics and Biodistribution of fPI-01 in Normal Nude Mouse

Prior to the application of the probe in tumor mice, the physiological behavior of the probe was firstly investigated in normal nude mouse (n=4). The background was imaged before probe administration. These mice were laid under the NIR imaging system after injection of 2 nmol of the probe in 0.1 ml saline. The entire real-time monitoring lasted for 8 h. The typical images were shown in Fig. 8a. At 10 min post-injection, the fluorescence probe mainly accumulated in liver, and weak fluorescence signal was observed in the bladder. While the fluorescence intensity in liver decreased, the signal in bladder increased with the time, as shown in the 30 min and 1 h image. After 8 h post-injection, the fluorescence intensity in liver and bladder decreased (As shown in Fig. 8a). During the real-time monitoring, the urine was imaged, as displayed in Fig. 8b. It was inferred that the probe firstly entered the liver and then excreted into urine by kidney.

To obtain more accurate information about the probe in the main organs, the subjected mice was sacrificed and anatomized at 8 h (n=4). Just after the abdomen was exposed, the mice body was imaged by the NIR imaging

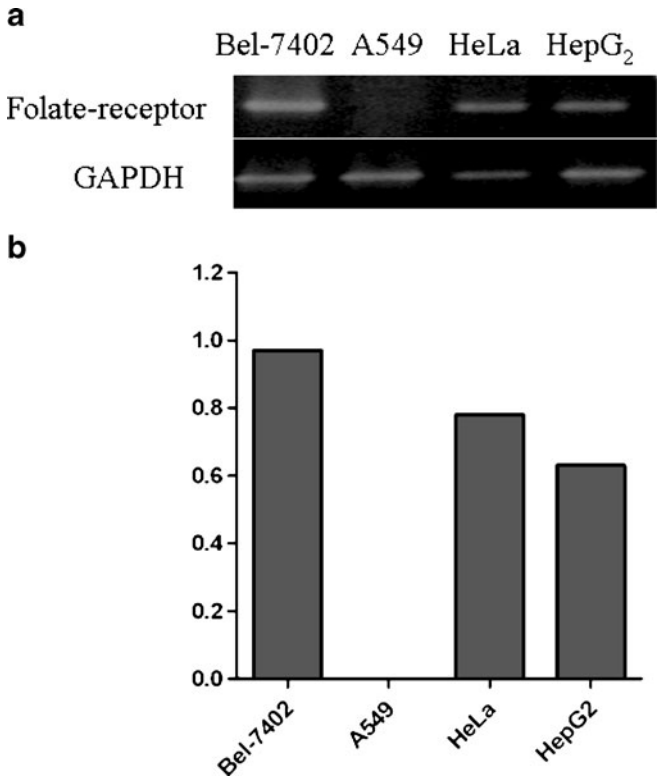

Fig. 6. mRNA level of folate-receptor was determined by reverse transcriptase PCR. **a** The products were analyzed by 2% agarose gel electrophoresis. **b** The *gray level* was analyzed.

system (As shown in Fig. 8c). More interestingly, the kidney was observed, which was not recognized during the *in vivo* monitoring before dissection. The reason should be that kidney laid below intestines and deep in the body. The fluorescence could not penetrate the thick tissues and be seized by the NIR imaging system.

Fig. 8d showed the fluorescence in the main organs extracted from the same mouse. After 8 h post-injection, fluorescence signal could only be seen in liver, kidney, and bladder. The other organs, including heart, lung, spleen, intestines, and testis, showed little fluorescence.

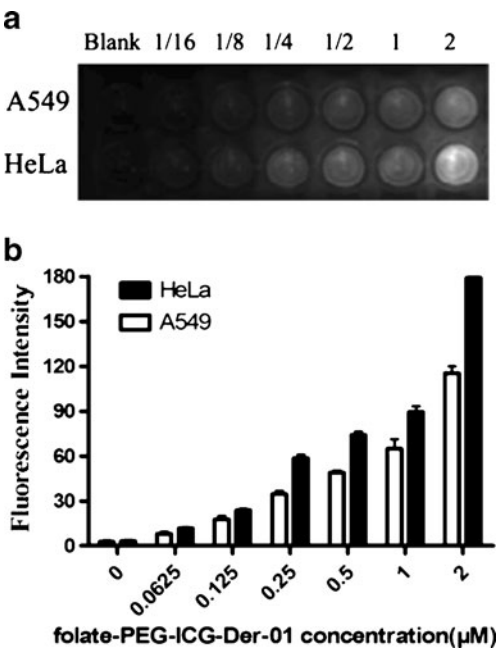

Fig. 7. Fluorescence intensity of HeLa and A549 cells solutions after treatment with fPI-01. Incubation 20 μl of fPI-01 in pH 7.2 PBS solution with blank, 1/16, 1/8, 1/4, 1/2, 1, and 2 μM for 1.5 h. **a** Image of the 96-well cell culture plate. **b** ROI analysis of fluorescence intensity from each well.

Targeted Capability of fPI-01 for Bel-7402 Tumor Xenograft Image Compared with ICG-Der-01

To investigate the tumor-targeted capability of fPI-01, the designed experiments were preformed in nude mice bearing Bel-7402 tumor xenograft in the right axillary fossa. Fig. 9 showed two typical series of NIR images after administration of ICG-Der-01 dye itself and fPI-01, respectively. In detail, Fig. 9a presented the typical images of a Bel-7402 tumor bearing mouse after ICG-Der-01 dye tail vein injection within 24 h. At the initial 10 s, the fluorescence signal spread all over the mouse, with the bright signal displayed in liver. The images at 2, 4, and 8 h displayed the fluorescence signal gradually moving to the abdomen, which was confirmed to be intestines by anatomic analysis (data not shown here). Since the bright fluorescence signal was also observed in dejecta, it was reasonably concluded that the ICG-Der-01 was cleared via the hepatobiliary route into the intestine, which was totally different from that of fPI-01 (Fig. 8a). During the entire monitoring period, the fluorescence did not display in the tumor site. It was implied that

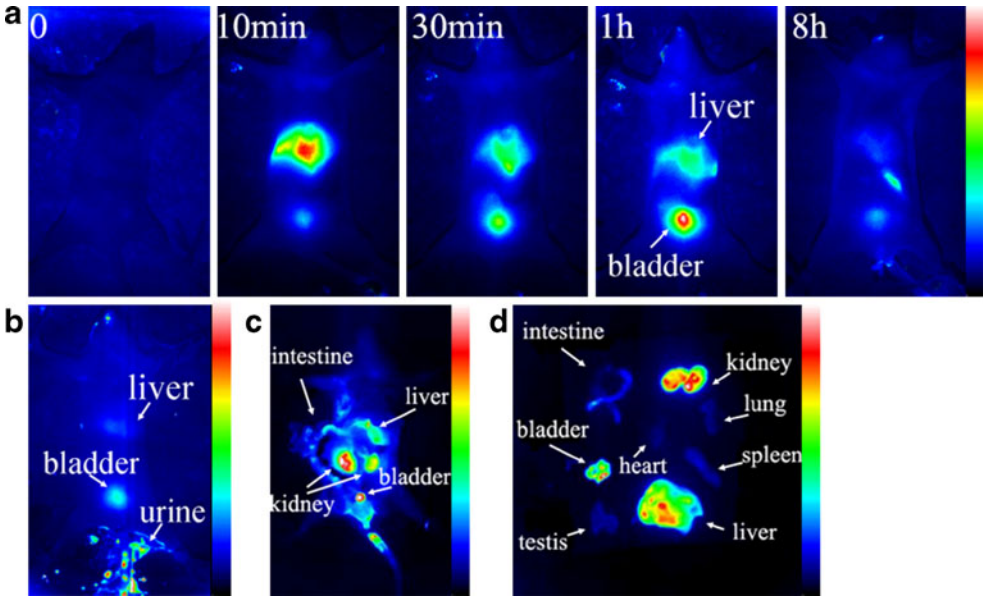

Fig. 8. Images of fPI-01 in normal mouse. **a** Non-invasive monitoring of the mouse after administration of the probe in 8 h. **b** Image of the urine. **c** Image of the main exposed organs. **d** Image of the main organs separated from the subjected mouse.

ICG-Der-01 itself did not possess the targeting capability to Bel-7402 tumor xenograft.

Fig. 9b exhibited the typical images of subjected mouse administrated with fPI-01. Similarly, the mouse was entirely bright at 30 s post-injection. The blood vessels in legs could be observed clearly. The brightest fluorescence signal was observed in liver. Gradually, the signals in liver decreased and excreted into urine by kidney. Tumor tissue was distinctly recognized at about 2 h after probe administration. The signal contrast ratio of tumor:normal tissue reached up to 20:1 at about 4 h post-injection. Fluorescence signal in tumor maintained bright even after 48 h post-injection. The tumor-targeting property demonstrated that fPI-01 is a satisfactory *in vivo* diagnostic agent for Bel-7402 tumor.

Determination of fPI-01 in Nude Mice Bearing Folate Receptor-Negative A549 Tumor Xenograft

The folate receptor-negative tumor was also used to determine the folate-targeting ability of fPI-01. Fig. 10 displayed a series of NIR images after fPI-01 was administrated into the subjected nude mice bearing A549 xenograft. The NIR images displayed the clear fluorescence signal firstly accumulated in liver and transported to the lower abdomen. At about 4 h, the bladder was clearly imaged and the urine also showed the intensive fluorescence signal. During the entire monitoring in 24 h, the A549 tumor tissue was weakly imaged but not very clear. Result implied fPI-01 showed weak targeting ability for folate-negative tumor *in vivo*.

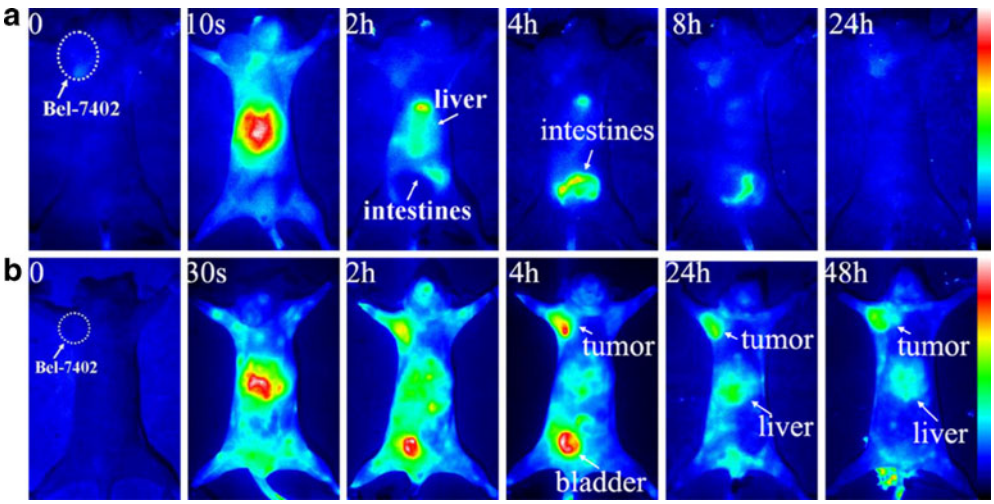

Fig. 9. NIR images of nude mice bearing Bel-7402 tumor xenograft. Folate-positive Bel-7402 tumor (0.5 ~ 0.7 cm) was implanted on the right axillary fossa. **a** Images of the mouse after administration of ICG-Der-01 within 24 h. **b** Images of the mouse after administration of fPI-01 within 48 h.

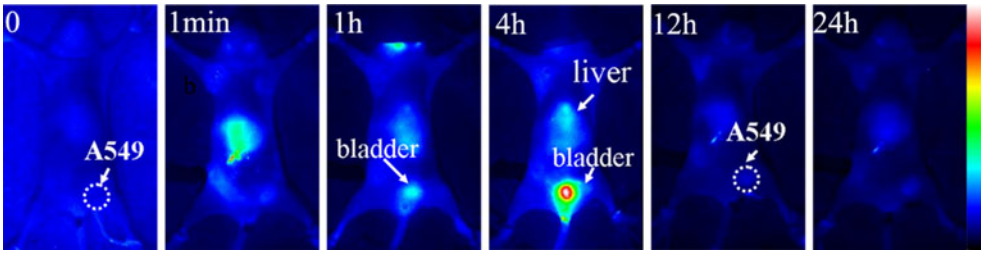

Fig. 10. Investigation of fPI-01 in nude mice bearing folate-negative A549 tumor xenograft. The A549 tumor was hazily imaged and a little fluorescence signal could be seen from the A549 tumor in the NIR images.

Targeting Sensitivity of fPI-01 in Little Unformed Tumor In Vivo

To determine the sensitivity of fPI-01 for *in vivo* early tumor diagnosis, the nude mice bearing little unformed HeLa tumor were used just after 4 days post-implantation (n=4). Fig. 11 showed the typical images of the subjected nude mouse. Interestingly, the little fluorescence spot where the cells were implanted (right lower fossa) was observed after about 20 min post-injection and was obviously distinguished from other tissue at about 1 h. The maximum signal contrast ratio reached to 10 at about 4 h post-injection. Signals in liver and bladder were also exhibited. That means the very early tumor stage can be detected as long as a certain amount of the tumor cells accumulated. This exciting finding demonstrated a prosperous potential for this compound to be used as very early malignant tumor diagnosis.

Further Investigation of the Targeting Affinity of fPI-01 in Other Two Tumor Models In Vivo

To extend the targeting capability of fPI-01 probe to folate receptor-overexpressed tumors, two kinds of other tumor models were used here, one with C6 tumor xenograft in left lower flank and the other with both $HepG_2$ and HeLa tumor xenograft on the right axillary fossa and lower flank, respectively (n=4). As shown in Fig. 12a, the C6 tumor in the subjected mouse was recognized at about 2 h post-injection and had the highest tumor:surrounding tissue ratio (5:1) at about 4 ~ 8 h. Fig. 12b displayed a series of typical images after fPI-01 administration into the subjected mouse bearing $HepG_2$ and HeLa xenografts. The $HepG_2$ and HeLa tumors were both imaged after 4 h post-injection. After 48 h, $HepG_2$ tumor exhibited better fluorescence signal ratio (9:1) than that of HeLa tumors (3:1). Fluorescence signal from the liver was always obtained during the entire monitoring.

Discussion

In this study, fPI-01 was successfully synthesized and characterized. The synthesized method was conducted in the formation of amide bond by DCC/NHS catalysis chemistry [42]. The fluorescence intensity of fPI-01 in pH 7.2 PBS was highly strengthened after ICG-Der-01 was conjugated with folate-PEG (As shown in Fig. 4c). The photostability of fPI-01 was obviously improved after conjugation. PEG is a hydrophilic polymer with higher water solubility and long circulation lifetime in living subjects. The solubility of ICG-Der-01 was strengthened after conjugated with PEG, which may highly improve the fluorescence intensity of the dye in water or pH 7.2 PBS. The macromolecules may act as a "protective umbrella" to hinder the dye from exposing to the high energetic laser. Thus, the chemical stability and photostability were also improved when ICG-Der-01 was conjugated with the soluble macromolecules. The improved high fluorescence intensity could make a reduced dose and an increased sensitivity for *in vivo* detection.

MTT assay was preferentially carried out in many experiments to evaluate the toxicity of a new compound [43]. In our study, the cell viability in MTT assay displayed totally above 88.2% and demonstrated the non-apparent cytotoxicity of the conjugated fluorescence probe (As shown in Fig. 5). In the new fluorescence compound, folic acid is actually vitamin B_{11} and plays important role in DNA synthesis. It is completely non-toxicity to the living cells and thus has been commonly used in many folate receptor-mediated targeting complexes as diagnostic and therapeutic

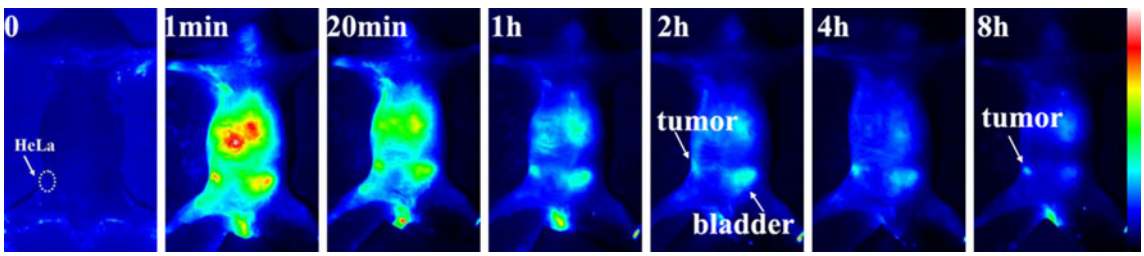

Fig. 11. NIR images of nude mice bearing little unformed tumor. HeLa cells were implanted on the right lower fossa. Tumor did not form after 4 days. The *little fluorescence spot* showed the location of tumor cells.

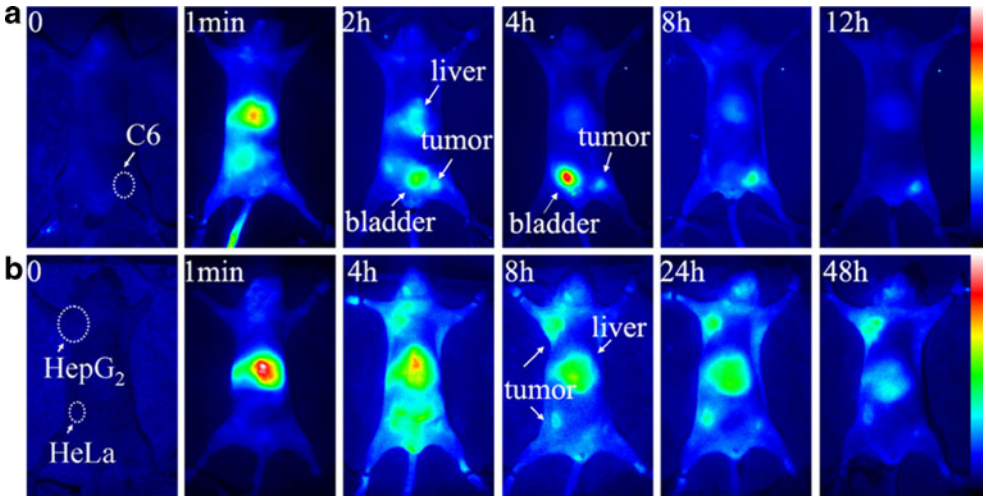

Fig. 12. NIR images of nude mouse bearing C6, both HepG2 and HeLa tumor after administration of fPI-01. **a** C6 tumor were implanted on the left lower flank, ~0.4 cm. **b** HepG2 and HeLa tumors were implanted on the right axillary fossa and lower flank for 4 weeks, ~0.8 and 0.5 cm, respectively. Fluorescence images of the mouse were acquired at different time intervals.

agents to cancers [5, 44]. PEG is a non-toxic agent and approved by FDA. PEG-modified agents have been abundantly developed and used in biomedicine [45]. ICG-Der-01 is a derivative of ICG, proved by FDA for human application. As a conjugation of the three non-toxic components, the final product was completely purified and the organic solvent used in synthesis was removed. That is the reason that fPI-01 in pH 7.2 PBS showed nearly no cytotoxicity in MTT assay. And the non-cytotoxicity of the probe makes it a potential agent for human subject.

fPI-01 was synthesized by derivating the carboxyl group of folic acid. However, folic acid has two carboxyl groups, α- and γ-carboxyl. And it was reported that folic acid retained its receptor-binding property when derived via its γ-carboxyl [5, 7, 44]. In our study, both carboxyl groups in folic acid may be probably activated by DCC/NHS. But the γ-carboxyl featured the priority of activation compared to the α-carboxyl. To ensure that the main product was γ-carboxyl derivation, we quantitatively controlled the addition of DCC/NHS (1.2/2) and the reaction temperature (50°C, 6 h) to avoid the α-carboxyl being activated. The single spot in thin layer plate assay indicated the one product achieved (As shown in Fig. 3a). In order to identify the folate receptor affinity of the probe, folate-positive HeLa and folate-negative A549 cells were cultured with different concentrations of the probe for 1.5 h, the lytic solution of HeLa cells showed higher fluorescence intensity than that of A549 cells (as shown in Fig. 6). The results demonstrated that folic acid remained its affinity for folate receptor in our synthesized probe, and the receptor-mediated endocytosis produced a marked effect on HeLa cells. It was implied that the synthesis of the probe did not obviously affect the chemical structure and physiological function of folic acid. However, the fluorescence signal was also observed from the lytic solution of A549 cells, which was previously considered as the folate receptor-negative cells (as shown in Fig. 6). The reason for fluorescence signal appeared in A549 cells should be further investigated.

The dynamics and biodistribution of fPI-01 were obtained by using NIR imaging system to monitor the fluorescence signal in the normal nude mice (n=4) after administration of fPI-01. And the subjected mice were sacrificed and main organs were separated to confirm the distribution. Just after the administration of the probe, the bright fluorescence was displayed all over the mouse, with blood vessel clearly observed in one minute. And then, the fluorescence signal accumulated in liver and moved to the bladder (Shown in Fig. 8a). Moreover, the urine displayed high fluorescence signal (Shown in Fig. 8b). The results showed the NIR fluorescence dye was eliminated by kidney after conjugated with PEG. It implied the eliminating routine of the probe is similar to PEG itself. The elimination routine by urinary system was also confirmed by the dissection, with high fluorescence signal in kidney and bladder at 8 h post-injection (as shown in Fig. 8c, d). The bright fluorescence signal in kidney after 8 h administration implied that normal kidney expressed certain amount of folate receptor [46]. Therefore, in many folate-targeted researches, the accumulation of small folate-targeted molecules in kidney was paid much attention. And the potential nephrotoxicity was highly concerned, especially for low molecular weight folate conjugates, such as folate radiopharmaceuticals, folate chemotherapeutics, and folate–hapten [47]. Though Müller reported preadministration of pemetrexed could significantly decrease the accumulation of folate-conjugated compound in kidney, the possible toxicity to kidney was still considered. Besides, it was also reported that the toxicity to kidney could be greatly prevented by using lager drug carries (>50 kDa) including polymers, nanoparticles, and micelles because they could not enter the cells in kidney [48]. In our study, a more hydrophilic,

biocompatible, and low toxical linker, PEG with molecular weight of 4,000 was used. Though the accumulation of fluorescence signal in kidney was observed (as shown in Fig. 8c, d), none of the mice in the study was killed after administration of the probe and the MTT assay indicated that the probe was nearly non-cytotoxicity (as shown in Fig. 5). Although there was not any apparent side effect being observed during the study, it was still requested that more researches should be carried out to identify whether the probe had some potential nephrotoxicity.

In the entire animal studies, all the NIR images showed there was an accumulation in liver just few seconds after injection of the probe and decreased many hours later (as shown in Figs. 8, 9, 10, 11, and 12). The fluorescence signal showed a long-term existence in liver, and the period was more than 48 h (as shown in Figs. 9 and 12). Fig. 8d approved the high intensity in the separated liver. It was inferred that the probe was metabolized in liver. Most of the metabolites excreted through the urinary system, as shown in Fig. 8b. The reason why the fluorescence signal existed longer in liver may be that the small amount of probe injected into the blood circulation was taken by Kupffer cells in liver, and the degradation may take a long time. More histological study should be carried out to determine whether there is certain extent of liver damage.

The most important characteristic of the probe we cared about was its targeting capability to tumor *in vivo*. The high affinity of folate as a targeting ligand to FA receptor over expressed tumors has been confirmed in many reports. Parker group characterized the expression level of folic receptors on several tumor lines by the quantitative radio-ligand binding assay [46]. According to Parker's evaluation and many reported papers, we selected the FR positive tumor lines (Bel-7402, HeLa, C6, HepG2 cell lines) to evaluate the targeting ability of our PEG-modified near infrared probes and its quick diagnostic potential. All the images demonstrated that fPI-01 was quickly accumulated in the FR positive tumor sites and can be used for the diagnosis of FR over expressed tumors.

Fig. 9 displayed a contrast experiment after administration of fPI-01 and ICG-Der-01 into nude mice bearing Bel-7402 tumor xenografts. It was clearly remarked that the tumor was accurately localized after administration of fPI-01, but ICG-Der-01 did not have the targeting ability. This contrast experiment depicted two main anticipated results: (1) ICG-Der-01 itself could not target to Bel-7402 tumor tissue; (2) the Bel-7402 tumor was accurately and clearly imaged by the folate-PEG conjugated ICG-Der-01 probe. The results demonstrated that fPI-01 is a high affinity agent to folate receptor and has great feasibility and practicability for *in vivo* tumor imaging.

A549 tumor cell line was selected as negative FR expression, Fig. 6 further confirmed its non-observable expression. The *in vivo* imaging in Fig. 10 also displayed a very weak signal in A549 tumor site. However, the little bright signals were still observed in Fig. 7 for the cell line *in vitro* experiments. The little bright signal may be due to the interaction of probe with the cells. The ambiguity *in vitro* experiment will motivate us to further investigate the interaction mechanism of fPI-01 with tumor cells.

The ability of the probe for early tumor diagnosis was also evaluated in a little unformed HeLa tumor model. The unformed tumors always cannot be distinguished from other normal tissues by using the ordinary imaging techniques. But the great growth velocity of tumor cells requires large quantities of nutrient substances. Folate is a kind of nutrient substance abundantly needed in the area of tumor cells and folate receptor is also overexpressed on the tumor cells. Thus, the folate-targeted probe could be accumulated in the spot where the tumor cells grow quickly. In our study, the little unformed tumor was imaged at the point where the HeLa cells were implanted just after 4 days (As shown in Fig. 11). The small fluorescence spot was quickly recognized at 30 min after administration of fPI-01. This phenomenon was not seen in other reports regarding tumor cells diagnostic agents. Our result demonstrated that fPI-01 could be quickly targeted to the place where tumor cells exist in the living body and the synthesized probe featured great potential in the diagnosis of early stage tumors.

We further evaluated the targeting property of the synthesized probe in other two folate receptor-overexpressed tumor models. The targeting capability of fPI-01 was attested again and the tumor tissues showed bright fluorescence signal (as shown in Fig. 12). The evaluation of the targeting property in the two tumor models demonstrated the potential capability of fPI-01 probe in the diagnosis of different kinds of tumors with positive folate receptor expression.

Conclusions

In summary, fPI-01 fluorescence probe was successfully synthesized and characterized in this study. The high affinity of the probe to the folate receptor-overexpressed tumor cells was verified by MTT assay. The targeting capability of the probe to folate receptor-overexpressed tumors was demonstrated in four different tumor models. In particular, the capability of the probe for early tumor diagnosis was confirmed in the unformed tumors. Results indicated that fPI-01 probe synthesized in this study is a promising NIR fluorescence imaging agents for the diagnosis of folate receptor-overexpressed tumors. The folate-PEG conjugation may become a potential molecular cargo for chemotherapeutics treatment. And the established technique in this study may also be used in evaluating tumor targeting capability of other drug carriers.

Acknowledgments. This research was supported by the Natural Science Foundation Committee of China (NSFC30371362, 30672015, 30700779, 30800257, 30970776) and the major project from the Ministry of Science and Technology for new drug development (2009ZX09310-004).

References

1. Okarvi SM, Jammaz IA (2006) Preparation and *in vitro* and *in vivo* evaluation of technetium-99m-labeled folate and methotrexate conjugates as tumor imaging agents. Cancer Biother Radiopharm 21:49–60
2. Leamon CP, Low PS (1991) Delivery of macromolecules into living cells: a method that exploits folate receptor endocytosis. Proc Natl Acad Sci (USA) 88:5572–5576
3. Guo W, Hinkle GH, Lee RJ (1999) ^{99m}Tc-HYNIC-folate: a novel receptor-based targeted radiopharmaceutical for tumor imaging. J Nucl Med 40:1563–1569
4. Yoo HS, Park TG (2004) Folate-receptor-targeted delivery of doxorubicin nano-aggregates stabilized by doxorubicin-PEG-folate conjugate. J Control Release 100:247–256
5. Leamon CP, Low PS (2001) Folate-mediated targeting: from diagnostics to drug and gene delivery. Drug Discov Today 6:44–51
6. Pan J, Feng SS (2009) Targeting and imaging cancer cells by Folate-decorated, quantum dots (QDs)—loaded nanoparticles of biodegradable polymers. Biomaterials 30:1176–1183
7. Siegel BA, Dehdashti F, Mutch DG et al (2003) Evaluation of ^{111}In-DTPA-folate as a receptor-targeted diagnostic agent for ovarian cancer: initial clinical results. J Nucl Med 44:700–707
8. Müller C, Schubiger PA, Schibli R (2007) Isostructural folate conjugates radiolabeled with the matched pair ^{99m}Tc/^{188}Re: a potential strategy for diagnosis and therapy of folate receptor-positive tumors. Nucl Med Biol 34:595–601
9. Sega EI, Low PS (2008) Tumor detection using folate receptor-targeted imaging agents. Cancer Metastasis Rev 27:655–664
10. Chen WT, Mahmood U, Weissleder R, Tung CH (2005) Arthritis imaging using a near-infrared fluorescence folate-targeted probe. Arthritis Res Ther 7:310–317
11. Zhou F, Xing D, Ou Z, Wu B, Resasco DE, Chen WR (2009) Cancer photothermal therapy in the near-infrared region by using single-walled carbon nanotubes. J Biomed Opt 14:021009
12. Reddy JA, Westrick E, Santhapuram HK et al (2007) Folate receptor-specific antitumor activity of EC131, a folate-maytansinoid conjugate. Cancer Res 67:6376–6382
13. Yamada A, Taniguchi Y, Kawano K, Honda T, Hattori Y, Maitani Y (2008) Design of folate-linked liposomal doxorubicin to its antitumor effect in mice. Clin Cancer Res 14:8161–8168
14. Pan J, Feng SS (2008) Targeted delivery of paclitaxel using folate-decorated poly (lactide)-vitamin E TPGS nanoparticles. Biomaterials 29:2663–2672
15. Douglas JT, Rogers BE, Rosenfeld ME, Michael SI, Feng M, Curiel DT (1996) Targeted gene delivery by tropism-modified adenoviral vectors. Nat Biotechnol 14:1574–1578
16. Luten J, van Steenbergen MJ, Lok MC et al (2008) Degradable PEG-folate coated poly(DMAEA-co-BA)phosphazene-based polyplexes exhibit receptor-specific gene expression. Eur J Pharm Sci 33:241–251
17. Thekkek N, Richards-Kortum R (2008) Optical imaging for cervical cancer detection: solutions for a continuing global problem. Nat Rev Cancer 8:725–731
18. Pierce MC, Javier DJ, Richards-Kortum R (2008) Optical contrast agents and imaging systems for detection and diagnosis of cancer. Int J Cancer 123:1979–1990
19. Weissleder R, Tung CH, Mahmood U, Bogdanov A Jr (1999) *In vivo* imaging of tumors with protease-activated near-infrared fluorescent probes. Nat Biotechnol 17:375–378
20. Mahmood U, Tung CH, Bogdanov A et al (1999) *In vivo* near-infrared fluorescence imaging of carcinoembryonic antigen–expressing tumor cells in mice. Radiology 213:866–870
21. Ogawa M, Regino CA, Choyke PL, Kobayashi H (2009) *In vivo* target-specific activatable near-infrared optical labeling of humanized monoclonal antibodies. Mol Cancer Ther 8:232–239
22. Björnsson OG, Murphy R, Chadwick VS (1982) Physiochemical studies of indocyanine green (ICG): absorbance/concentration relationship, pH tolerance and assay precision in various solvents. Experientia 38:1441–1442
23. Zou P, Xu S, Povoski SP et al (2009) Near-infrared fluorescence labeled anti-TAG-72 monoclonal antibodies for tumor imaging in colorectal cancer xenograft mice. Mol Pharm 6:428–440
24. Xiao W, Yao N, Peng L, Liu R, Lam KS (2009) Near-infrared optical imaging in glioblastoma xenograft with ligand-targeting alpha3 integrin. Eur J Nucl Med Mol Imaging 36:94–103
25. Chen X, Conti PS, Moats RA (2004) *In vivo* near-infrared fluorescence imaging of integrin αβ3 in brain tumor xenograft. Cancer Res 64:8009–8014
26. Yamamoto Y, Tsutsumi Y, Yoshioka Y et al (2003) Site-specific PEGylation of a lysine-deficient TNF-alpha with full bioactivity. Nat Biotechnol 21:546–552
27. Zhang S, Zhang Y, Liu J, Zhang C, Gu N, Li F (2008) Preparation of anti-sperm protein 17 immunomagnetic nanoparticles for targeting cell. J Nanosci Nanotechnol 8:2341–2346
28. Tung CH, Lin Y, Moon WK, Weissleder R (2002) A receptor-targeted near-infrared fluorescence probe for *in vivo* tumor imaging. Chembiochem 8:784–786
29. Stefflova K, Li H, Chen J, Zheng G (2007) Peptide-based pharmacomodulation of a cancer-targeted optical imaging and photodynamic therapy agent. Bioconjug Chem 18:379–388
30. Ye Y, Bloch S, Kao J, Achilefu S (2005) Multivalent carbocyanine molecular probes: synthesis and applications. Bioconjug Chem 16:51–61
31. Qian H, Gu Y, Wang M, Achilefu S (2009) Optimization of the near-infrared fluorescence labeling for *in vivo* monitoring of a protein drug distribution in animal model. J Fluoresc 19:277–284
32. Furukawa S, Katayama N, Iizuka T et al (1980) Preparation of polyethylene glycol-bound NAD and its application in a model enzyme reactor. FEBS Lett 121:239–242
33. Chen H, Zhang J, Qian Z et al (2008) *In vivo* non-invasive optical imaging of temperature-sensitive co-polymeric nanohydrogel. Nanotechnology 19:185707–185717
34. Hong G, Yuan R, Liang B, Shen J, Yang X, Shuai X (2008) Folate-functionalized polymeric micelle as hepatic carcinoma-targeted, MRI-ultrasensitive delivery system of antitumor drugs. Biomed Microdevices 10:693–700
35. Kam NW, O'Connell M, Wisdom JA, Dai H (2005) Carbon nanotubes as multifunctional biological transporters and near-infrared agents for selective cancer cell destruction. Proc Natl Acad Sci (USA) 102:11600–11605
36. Kang B, Yu D, Chang S, Chen D, Dai Y, Ding Y (2008) Intracellular uptake, trafficking and subcellular distribution of folate conjugated single walled carbon nanotubes within living cells. Nanotechnology 19:375103–375111
37. Hsu AR, Hou LC, Veeravagu A et al (2006) *In vivo* near-infrared fluorescence imaging of integrin alphavbeta3 in an orthotopic glioblastoma model. MolImaging Biol 8:315–323
38. Destito G, Yeh R, Rae CS, Finn MG, Manchester M (2007) Folic acid-mediated targeting of cowpea mosaic virus particles to tumor cells. Chem Biol 14:1152–1162
39. Zhang J, Chen H, Xu L, Gu Y (2008) The targeted behavior of thermally responsive nanohydrogel evaluated by NIR system in mouse model. J Control Release 131:34–40
40. Chen H, Wang Y, Xu J et al (2008) Non-invasive near infrared fluorescence imaging of CdHgTe quantum dots in mouse model. J Fluoresc 18:801–811
41. Ryan SM, Mantovani G, Wang X, Haddleton DM, Brayden DJ (2008) Advances in PEGylation of important biotech molecules: delivery aspects. Expert Opin Drug Deliv 5:371–383
42. Lee ES, Na K, Bae YH (2003) Polymeric micelle for tumor pH and folate-mediated targeting. J Control Release 91:103–113
43. Leamon CP, Reddy JA, Vlahov IR, Kleindl PJ, Vetzel M, Westrick E (2006) Synthesis and biological evaluation of EC140: a novel folate-targeted vinca alkaloid conjugate. Bioconjug Chem 17:1226–1232
44. Leamon CP, Reddy JA (2004) Folate-targeted chemotherapy. Adv Drug Deliv Rev 56:1127–1141
45. Kim BK, Kwon SY, Ko SY et al (2008) Treatment with pegylated interferon and ribavirin in a patient with fibrosing cholestatic hepatitis due to recurrent hepatitis C after liver transplantation. Korean J Hepatol 14:519–524
46. Parker N, Turk MJ, Westrick E, Lewis JD, Low PS, Leamon CP (2005) Folate receptor expression in carcinomas and normal tissues determined by a quantitative radioligand binding assay. Anal Chem 338:284–293
47. Low PS, Henne WA, Doorneweerd DD (2008) Discovery and development of folic-acid-based receptor targeting for imaging and therapy of cancer and inflammatory diseases. Acc Chem Res 41:120–129
48. Zhao X, Li H, Lee RJ (2008) Targeted drug delivery via folate receptor. Expert Opin Drug Deliv 5:309–319